

A COMPUTATIONAL MODEL OF NERVE SIGNAL DETECTION AND RECOGNITION DURING VOLUNTARY MUSCLE CONTRACTIONS

Rui Zhou, Ning Jiang, Kevin Englehart, Philip Parker
University of New Brunswick, Fredericton, N.B., Canada

INTRODUCTION

Myoelectric signals (MES), which are generated by muscle contraction, are utilized in myoelectric control of powered upper-extremity prostheses. This is an effective and noninvasive method, for individuals with amputations or congenitally deficient upper limbs [1]. The MES has unique patterns containing the contraction information and correspondingly can be extracted in the form of feature vectors. Therefore, pattern recognition techniques have been extensively used as effective methods for myoelectric control [2][3].

The MES can be recorded by surface electrodes or needle electrodes, placed at several muscle sites [4]. Although the MES has been used for myoelectric control for many years, inherent characteristics limit their efficacy in wider use. Surface electrodes have limited information due to the fact that they cannot measure the contribution from deep muscles; moreover, the pick-up areas of surface electrodes are rather large, thus identifying information from certain target muscles is difficult due to crosstalk from adjacent muscles. Embedded electrodes, such as needle electrodes, solve those problems to a certain extent. Their recording areas are much smaller, thus, due to the small structure, they can be inserted into any target muscle to provide localized signals. Their use in myoelectric control however is confounded by the sensitivity to electrode position, and the practical difficulties of chronic implantation.

This paper presents a novel model to investigate the information content about voluntary movement, based on the signals from active nerves. Differing from the myoelectric methods, this investigation provides a simulation of the information obtained by picking up the signals from relevant functional nerve fascicles, rather than muscles, during volitional intent. This approach avoids the crosstalk and overcomes the problem of recording from deep muscles.

METHODOLOGY

Microsurgery and microneurography have revealed a fascicular grouping in peripheral nerves [5]. The location, morphology, and number of nerve fascicles were observed from a series of cross-sections along

the nerve course, and the topographic maps were drawn to show the varying geometric positions of motor neurons, sensory nerves, or assorted nerves in nerve bundles.

Sunderland established the fundamental theory of somatotopic organization of the peripheral nerve system in 1945 [6][7][8]. More recently, experiments have involved histochemical approaches, intraneural microstimulation [10], and many other methods to provide more substantiated information, including histological structure of nerves, number of nerve fibres, anatomical variation, and terminal points. We can now be very confident that fibres group to specific muscles or specific skin areas as fascicles or within fascicles, and even in the very proximal parts of the nerves, they do not intermingle considerably [11].

In this paper, at the positions where target functional nerve branches can be clearly identified, a computational nerve model is described that can simulate the nerve signals. When muscles contract, the activities from innervating nerves are "recorded"; additionally, if some muscles are innervated by more than one functional branch, primary and subordinate branches are all taken into account, within hierarchical active fiber subsets. By use of arrays such as the Utah Slanted Electrode Array (USEA), signals can be recorded from selected branches.

Choice of motions and recording sites

The required musculature was specified to satisfy the independent control of a two degree-of freedom wrist, and 3 two degree-of freedom prosthetic hand [12]. The independent intra-muscular EMG can be acquired from the following muscles in the forearm: supinator teres (ST) and pronator teres (PT) for wrist rotation; flexor carpi ulnaris (FCU) and extensor carpi ulnaris (ECU) for wrist flexion and extension; and flexor digitorum sublimis (FDS) and extensor digitorum communis (EDC) for finger opening and closing [13]. Therefore, the corresponding functional nerve branches are chosen in this case.

1) Anatomic Analysis of the Median Nerve (MN):

The internal topographic fiber distribution of the median nerve has been extensively studied in the literature; the fascicles consistently assemble into three

Table 1 Branch Compositions of the three Fascicular Groups of the Median Nerve in Thirty-four Arms

Group	Pronator Teres	Portion of Branch Entering Flexor Digitorum Superficialis*		
		Proximal	Middle	Distal
Anterior	34			
Posterior		16		
Middle		1	34	34
Total#	34	17	34	34

* The branches entering the muscles by the middle portion were the major branches; # Branches that were seen in fewer than thirty-four arms were fine and inconstant.

groups, located at anterior, middle, and posterior parts of the nerve trunk [14]. The PT branch resides in the anterior group, and the FDS is one of the branches of the middle group. Even though the fibres of those branches separately innervate different terminal points along the nerve course, somatotopic organization of the three groups remain quite distinct in a series of cross-sections. The position of the cross-section is chosen at the distal 1/8 of the arm, where the functional branches can be split atraumatically (Table 1) [14].

Histomorphologic data of the nerve show the number of fibres for each branch and the total fascicular areas of them (Table 2) [5].

2) Anatomic Analysis of the Ulnar Nerve (UN):

The ulnar nerve innervates the FCU and part of the flexor digitorum profundus muscle (FDP) in the forearm. As the innervating nerve of the flexor carpi ulnaris muscle, the FCU branch in the ulnar nerve diverges between 13/16 of the forearm and the distal 1/8 of the arm, mostly located at the posterior or posterolateral part with the 1/6 area of the nerve trunk, so the dissection place can be chosen between the 14/16 of the forearm and the level of the medial epicondyle. Even though the group intermingles with neighboring

Table 2 Median Nerve: Histomorphologic Data (n=15)

Nerve	No. of Fibres Δ	No. of Fascicles	Total Fascicular Area(mm ²)
Pronator Teres			
Proximal	476	1	0.075
Middle	769	1	0.12
Distal	933	2.5	0.155
FDS			
Proximal	1616	4.5	0.22
Distal	1313	2	0.3

Δ Total number of myelinated fibres.

fascicles, the majority of its fibres are still located at the posterolateral part of the trunk when it develops to the proximity [16] [17]. The nerve properties of the FCU branch have been identified in Mackinnon's work [18]. The mean total fibre numbers within the FCU branch is 700 approximately; the mean cross-section area is 142,492 μm^2 (SEM=19,633 μm^2) [18]. The mean area of ulnar nerve is set to be 8.6 mm².

3) Anatomic Analysis of the Radial Nerve (RN):

Although the bifurcating positions of nerves vary in different subjects, most investigations show that, starting from the distal 1/8 of the arm, the superficial branch and the deep motor branch of the radial nerve have no identifiable intra-fascicular intermingling [24][25][26]. Therefore, in this case, the dissecting place is chosen to be at the distal 1/8 of the arm, 25.4 mm proximal to the lateral humeral epicondyle. The EDC and ECU branches both originate from the Posterior Interosseous Nerve (PIN), which occupies the posterior 2/3 area of the radial nerve, and the ST is split from the PIN as well. It is known that the mean cross-section area of the radial nerve trunk is 4.70 \pm 0.27 mm², and 8.5% is occupied by the ST while the EDC and ECU take 13.5% of the area [24][8]. According to the previous research on PIN, 6 branches are given off and distributed from ulnar to radial side at their origins [27]. The first and second branches, at the ulnar side, innervate the EDC; the third innervates the ECU; the sixth gives rise to three new branches, and the most radial of these innervates the ST [27]. The mean fascicle numbers of ST, EDC, and ECU nerve branches are 3.9 \pm 1.4, 4.6 \pm 1.3, and 2.8 \pm 0.8, respectively [26].

Apparatus

Instead of modeling surface electrodes or regular intramuscular approaches, this investigation models the recording response of the USEA as a representation of the signals from selected nerve fibres.

Experimental studies have shown that the USEA can be implanted into multiple nerve fascicles to record signals from independent subpopulations of motoneurons which innervate the intrinsic muscles [19]. The USEA consists of a 10x10 grid of electrodes spaced by 400 microns, projecting from a 4 mm by 4 mm silicon substrate, and the electrode length of each row varies linearly from 0.5 cm to 1.5 cm [20][21]. The unique structure successfully integrates many electrodes to be used in 3-dimensional signal recording. In preliminary experiments, the USEA has been proved to be highly selective and have good biocompatibility without chronic histological damage or unacceptable fibrous encapsulation [23].

A Case Study

Wrist Pronation is mainly controlled by the PT muscle, so the PT nerve branch is regarded as the only innervating nerve in this case. The PT nerve branch is located within the anterior group of the median nerve, with a cross-sectional area equaling 0.1167 mm^2 . The radius of median nerve trunk is set to be 1.5 cm [23].

The distance between each cross section among the serial divisions in the arm (every $1/8$ length of the arm [23]), is 25.4 mm, which is evidently longer than the length of the USEA (4 mm). Consequently, we assume a topographical distribution within the generated nerve bundle remains consistently at the chosen level and its adjacent area, which is the area the USEA covers.

The figure below shows the cross-section of the generated PT nerve branch with one USEA inserted, to represent the intra-neural topographic insertion of the USEA.

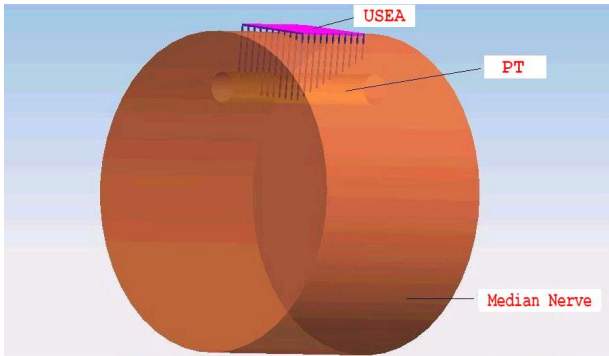


Figure 1 Intra-neural graph of a USEA in the MN

Simulation

Two seconds of the action potential trains for each contraction are generated at a 5 kHz sampling frequency, and the inter-pulse interval of the action potential train is a random process (Gaussian, with a mean of 50 ms, and a coefficient of variation of 15%).

By selectively activating the subpopulation of the target nerves at designated percentages, electrodes detect the action potential trains from the active fibres within their 200 micron recording distance, taking into account of the tissue attenuation effect. Preliminary work has shown that the amplitude of detected signals decreases in inverse proportion to the recording distance:

$$\text{Amp}_{\text{recorded}} = 1/(\text{Recording distance})^P, \quad (P > 0) \quad (1)$$

By fitting the curve of the electrode recording distance effect, as found in [28], the attenuation coefficient P is determined to be 1.9.

Based upon the anatomical information of nerve fascicles such as density, the number of fibres, and

geometric position, six nerve branches have been simulated: FDS (hand closing, wrist flexion), EDC (hand open and wrist extension), FCU (wrist flexion), ECU (wrist extension), PT (wrist pronation), and ST (wrist supination). Nerve fibres in these fascicles are assumed uniformly distributed. As a first-order approximation, it is assumed that primary nerves have 70% of fibres activated (or course, the exact level of motor nerve recruitment depends upon the intensity of contraction). During wrist flexion/extension, FDS and EDC are 20% activated when they are behaving as secondary nerves. After generating these target nerve branches, every active fibre will generate an action potential train. Each fibre is unique and independent of the others, avoiding the interference of signal crosstalk.

In order to completely cover the fascicles of interest, four USEAs are employed in the signal detections of the fascicles, two for the MN, one for the RN, and the other for the UN. The obtained signal is the summation of the signal that each electrode detects within its recording distance.

Figure 2 shows the mean square value (MSV) of recorded signals from channels of the USEA during six voluntary contractions (hand closing/ open, wrist extension/flexion, and wrist pronation/supination), each lasting for 2 seconds. There are distinct patterns across the six contractions.

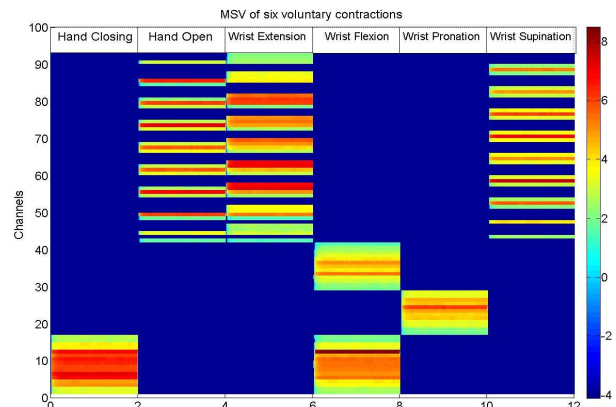


Figure 2 MSV of action potential signals across six voluntary contractions

CONCLUSION

This paper demonstrates a new approach to extracting muscle contraction information based on a computational nerve model. As discussed above, since the somatotopic organization and topographic distribution in nerve bundles, and other anatomical information are well defined in the literature, we are able to simulate the nerve models with these properties, and use it with statistical innervating sequences (six

muscle contractions). The anatomical dissection locations are distal to the level of median and lateral epicondyle, so the model is suitable for representing the data acquired from an above-elbow amputee.

Since the signals are all generated from the specific branches directly when corresponding muscles are innervated, information can be drawn with specificity from the relevant nerves. Acquiring these data from nerves eliminates the problems of accessing deep muscles and signal crosstalk when using the surface MES. Therefore, this model circumvents the limitation in surface MES analysis. Furthermore, it can be customized to any muscle contraction, including superficial and deep muscles. This model shows the distinctly different nerve activation patterns across motion types.

This model is in its initial development, without consideration of any noise or signal degradation due to electrode encapsulation, but these will be integrated in future development. The goal is to build a model which can provide a complete description of neural activity during voluntary intent, by recordings of the USEA at all sites of the forearm nerves. The coincident MES activity, as acquired from the surface of the forearm, can be generated simultaneously. This will allow a direct comparison of the information content in peripheral nerves as compared with the surface EMG, which will provide an effective means of evaluating the design requirements of peripheral nerve interfaces for prosthetic control, with regard to the number of arrays, the placement of these arrays, and the number and geometry of electrodes on each array.

REFERENCES

- [1] R.N.Scott, P.A.Parker, Myoelectric prostheses: State of art, *J.Med. Eng. Tech.*, Vol. 12, pp.143-151, 1988
- [2] K.Englehart, B. Hudgins, A robust, real-time control scheme for multifunction myoelectric control, *IEEE Trans. Biomed. Eng.*, Vol. 50, No. 7, pp. 848-854, 2003
- [3] D.Dorcas, R.N.Scott, A three state myoelectric control, *Med. Biol. Eng.*, Vol. 4, pp.367-372, 1966
- [4] I.Gath, E.Stalberg, Techniques for improving the selectivity of electromyographic recordings, *IEEE Trans. Biomed. Eng.*, Vol. BME-23, No.6, pp. 467-472, 1976
- [5] J.D. Stewart, Peripheral nerve fascicles: anatomy and clinical relevance, *Muscle Nerve*, Vol.28, pp.525-541, 2003
- [6] S.Sunderland, Intraneural topography of radial, median and ulnar nerves, *Brain*, Vol.68, pp. 245-299, 1945
- [7] S.Sunderland, *Nerves and nerve injuries*, Edinburgh: Churchill Livingstone, 1978
- [8] S.Sunderland, Numbers of nerve fibers for individual branches, *Nerve injuries and their repair: a critical appraisal*, pp. 41-45, 1991
- [9] F.Bonnel, Microscopic anatomy of the adult human brachial plexus: An anatomical and histological basis for microsurgery, *Microsurgery*, Vol. 5, Issue 3, pp. 107-117, 1984
- [10] W.Schady, J.L.Ochoa, H.E.Torebjork, Peripheral projections of fascicles in the human median nerve, *Brain*, Vol. 106, Issue 3, pp. 745-760, 1983
- [11] W.Johnston, J.D.Stewart, Sciatic neuropathies: a 10 year experience, *Can. J. Neurol. Sci.*, pp. 17-249, 1990
- [12] R.F.ff.Weir, Design of a clinically viable multifunctional prosthetic hand, *Myoelectric Controls Conference (MEC2002)*, Fredericton, New Brunswick, Canada, 2002
- [13] R.F.ff.Weir, P.R.Troyk, G.DeMichele, T.Kuiken, Implantable myoelectric sensors (IMES) for upper-extremity prosthesis control—preliminary work, pp. 1562-1565, *Proc. 25th Annu. Int. Conf. IEEE EMBS*, Cancun, Mexico, 2003
- [14] X.Zhao, J.Lao, L.Hung, G.Zhang, L Zhang, Y.Gu, Selective neurotization of the median nerve in the arm to treat brachial plexus palsy, *The Journal of Bone and Joint Surgery*, Vol. 86-A, No. 4, pp. 736-742, 2004
- [15] T.H.Tung, S.Mackinnon, Flexor digitorum superficialis nerve transfer to restore Pronation: two case reports and anatomic study, *J. Hand Surg.*, Vol. 26A, pp.1065-1072, 2001
- [16] S.Li, L.Gu, Y.Shao, T.Sun, Distribution and localization of fascicular groups to intrinsic muscles of ulnar nerve trunk, *Chin. J. Clin. Rehab.*, Vol. 10, No. 24, pp. 117-119, 2006
- [17] S.Zhong, M.Liu, Y.Tao, A study of the microsurgical anatomy of the ulnar nerve, *ACTA Anatomy Sinica*, Vol. 12, No. 4, pp. 346-354, 1981
- [18] S.E.Mackinnon, Transfer of flexor carpi ulnaris branch of the ulnar nerve to the pronator teres nerve: Histomorphometric analysis, *J. Recon. Microsurg.*, Vol. 12, No. 2, pp. 119-122, 1999
- [19] R.Normann, D.McDonnall, G.Clark, R.Stein, A.Branner, Physiological activation of the hind limb muscles of the anesthetized cat using the Utah slanted electrode array, *Proc. Intl. Joint Conf. on Neural Networks*, Montreal, Canada, 2005
- [20] A.Branner, R.Stein, R.Normann, Selective stimulation and recording using a slanted multielectrode array, *Proc. of the first Joint BMES/EMBS Conf.*, Atlanta, GA, USA, 1999
- [21] P.Rousche, R.Normann, Chronic intracortical microstimulation (ICMS) of cat sensory cortex using the Utah intracortical electrode array, *IEEE Trans. Rehab. Eng.*, Vol. 7, No. 1, pp. 56-68, 1999
- [22] P.Rousche, R.Normann, Chronic recording capability of the Utah intracortical electrode array in cat sensory cortex, *J. Neuroscience Method*, Vol. 82, Issue 1, pp. 1-15, 1998
- [23] S.Zhong, M.Liu, J.Zhu, A study of the microsurgical anatomy of the median nerve, *ACTA Anatomy Sinica*, Vol. 11, No. 4, pp. 337-346, 1980
- [24] S.Zhong, M.Liu, C Zhu, Y.Tao, A study of the microsurgical anatomy of the radial nerve, *ACTA Anatomy Sinica*, Vol. 14, No. 1, pp. 1-7, , 1983
- [25] T.Huang, D.Liu, J.Qin, An anatomical study of muscular branches of radial nerve in the forearm, *Chin. J. Orthop.*, Vol. 22, No. 3, pp. 158-160, 2002
- [26] R.A.Abrams, R.J.Ziets, R.L.Lieber, M.J.Botte, Anatomy of the radial nerve motor branches in the forearm, *J. Hand Surg.*, Vol. 22A, No. 2, pp. 232-237, 1997
- [27] H.ElGafy, N.Ebraheim, R.Yeasting, The anatomy of the posterior Interosseous nerve as a graft. *J. Hand Surg.*, Vol. 25A, No. 5, pp. 930-935, 2000
- [28] Ekstedt,J., Stalberg, E., How the size of the needle electrode leading off surface influences the shape of the single muscle fibre action potential in electromyography, *Comput Progr Bimed*, Vol. 3, Issue 4, pp. 204-212, 1973